Characterisation of the far field pattern for plastic optical fibres

M. A. Losada, J. Mateo, D. Espinosa, I. Garcés, J. Zubia*
University of Zaragoza, Zaragoza (Spain)
*University of Basque Country, Bilbao (Spain)

Abstract

In this paper, we present an imaging system designed to register the spatial distribution of the optical power at the exit of the fibre (far field pattern) for plastic optical fibres (POFs). The final aim of this work is to study the variation of the far field pattern (FFP) with fibre length and for different conditions of light injection. Modal interaction is the mechanism underlying the shape of the power distribution and thus, the analysis of these images can help the understanding of the fibre modal behaviour. In particular, we introduce several methods to describe the FFP profiles and we obtain the exit numerical aperture (NA) of the fibre using different approaches.

Introduction

The shape of the far field pattern (FFP) of the power distribution at the output of a POF is determined by the fibre modal distribution, which depends on fibre length, launching conditions and coupling strength of the fibre. Since modal distribution is related to fibre bandwidth through modal dispersion, a better knowledge of the behaviour of the FFP with length will contribute to a better understanding of bandwidth, especially at short lengths when the modal equilibrium has not been reached. Indeed, there are studies that postulate that bandwidth can be estimated from the fibre exit numerical aperture (NA) [1, 2] that has to be calculated from the measured FFP profile for each condition.

In the Japanese Industrial Standard (JIS) [3], there are several methods recommended to obtain the NA of a POF, but the most generally used is that based on the FFP formed at a sufficiently large distance from the output of the fibre. FFPs are usually obtained by a scanning method with a single detector or using a one-dimensional (1D) array of detectors. Both systems provide only 1D information of the FFP which is sufficient to obtain the NA as the sine of the acceptance angle defined as the angle for which the power decreases at 5% of its maximum.

Here, we propose a method based on a CCD camera to obtain directly the FFP from two-dimensional (2D) images. This method has several advantages over the previous ones. First, it is faster than the scanning method. Second, it does not need the vertical pre-aligning of the detecting system and the fibre axis to find the FFP central diameter. Third, it produces 2D images rather than 1D profiles which make the method more robust. In addition, in a recent study [4], we observed that images with different profile shapes may produce similar NA values. Thus, we concluded that a single parameter, the NA, may be not enough to describe the FFP profile and to explain the modal behaviour of POFs. Therefore, here we introduce a model to fit the shape of the FFP by means of generalised "Super-Gaussian" functions that take into account its variable kurtosis. From the 2D, we estimate the NA using different approaches in order

to determine what method is more precise and robust, and we validate our results by comparing them with the JIS scanning method.

As an application of this method, we have measured the NA versus length for a high NA fibre for four different launching conditions. Our future aim is to assess the dependence of exit NA with launching conditions and fibre length, and compare it with the dependence found for bandwidth to determine their relationship.

Experimental methods and procedures

1. Experimental System:

We used a 12 bit monochrome cooled camera QICAM FAST 1394 to register FFP images reflected on a white screen situated 108mm from the fibre exit end. The fibre was placed into a holder specifically designed to have its end surface precisely over the centre of a rotating stage that allows output angle scan. Thus, the fibre end will be always in the same position which will be crucial to compare data obtained with different conditions. The size of the CCD was 1392x1040, but the images were taken with a 4x4 binning so the image size was in fact 384x260 pixels. The distance of the camera to the screen was set at 550mm. To avoid the blocking effect of the fibre holder, the camera had to be tilted 34 degrees from the axis perpendicular to the screen as shown in the scheme of this set-up, depicted in Figure 1. The distortion due to the tilt was obtained by imaging a pre-calibrated pattern, and corrected as soon as the image is captured. The whole acquisition block was mounted on an optical table and covered by a box to avoid external light. Behind the screen, a large-area silicon detector with a pinhole mask was introduced in order to measure the output power versus the output angle, which is necessary to compare our method with the standard.
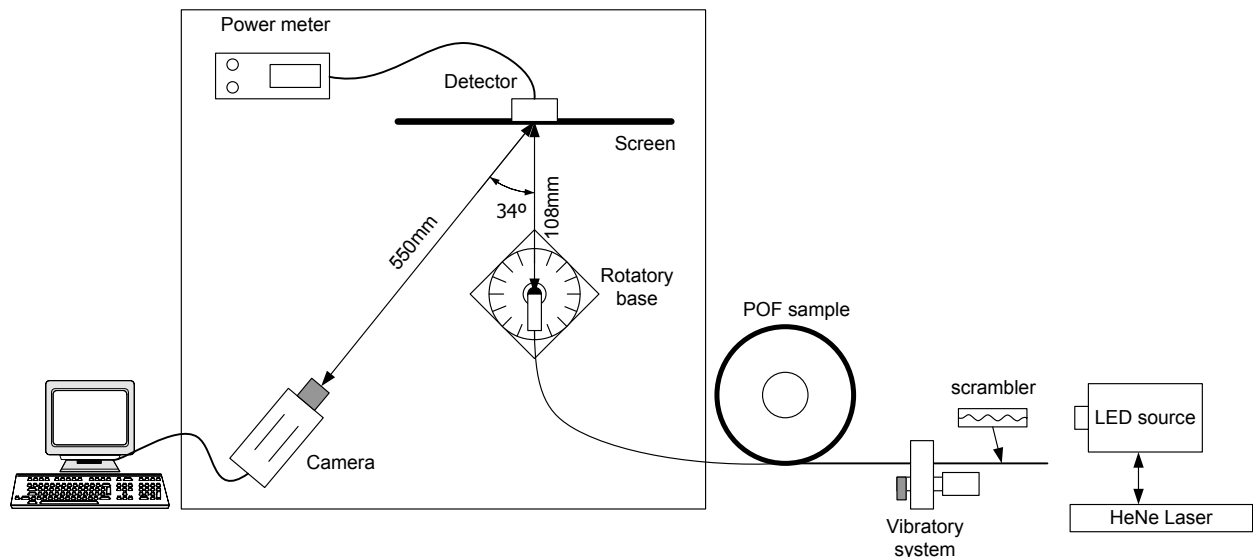

Figure 1: Experimental set-up to register the FFP images of a POF.

The image acquisition was controlled by software designed specifically using LabView™ to display the FFP image with the correct spatial scale and perspective, and to extract different characteristics in real time. The parameters required for image capture, such as camera aperture, exposure time and gain were fixed after a previous analysis of the power balance. For each condition, the background image was taken,

and subtracted on line from the corresponding FFP images. The radial, horizontal and vertical profiles were extracted from the raw images, which were no filtered or enhanced intentionally to compare between different NA estimates from different methods.

Using the described set-up, we have obtained the FFP images versus length using two different sources: A He-Ne laser emitting at 633nm with a very small divergence, and a light emitting diode (LED) from Fotec at 665nm with a NA=0.3. The He-Ne laser was launched directly on the fibre, and the LED was provided with a built-in connector. In addition, a scrambler was inserted near the input end of the fibre to achieve higher NA launching conditions for both sources. This scrambler has been thoroughly described elsewhere [5]. When we used the laser as the source, the images on the screen presented considerable speckle noise. The speckle noise was minimised with a mechanical vibration generated by an external motor and applied to the fibre near the input end as described in [6].

The fibre used was PGU-CD1001-22E from Toray with nominal NA of 0.5. The experimental procedure was as follows. We started with a 64m segment rolled onto an 18cm diameter reel. The launching conditions tested were the following: He-Ne laser without scrambler, LED without scrambler, He-Ne laser with the corrugated scrambler at the input end and LED with the scrambler at the input end. After recording the 4 images corresponding to these conditions, a segment of 2.5m was cut from the scrambler end, which was always at the input end of the fibre to maintain the same output termination through all the experiment.

2. Characterisation of the FFPs and NA estimation:

Our aim is to find a complete characterisation of the shape of the FFP profiles, and also a robust estimate of the exit NA of the fibre. We have studied two different methods to characterise the FFP profiles and several approaches to obtain the NA. First, after obtaining the image centroid, the horizontal profile was extracted as the horizontal row containing the vertical coordinate of the centroid, and the radial profile was calculated by averaging the values of all the pixels at a given distance from it. Thus, the NA was calculated from the acceptance angle obtained directly from the raw data of both the horizontal and radial profiles.

In addition, we introduced a method based on 2D data and presumably more robust than the others. In this method, a threshold was applied over the 2D image to select the pixels with higher power than a given percentage of the maximum (95%, 90%, 50%, 10%, 5%) and the area of the circle including the pixels was obtained. Its radius gives a robust estimate of the width of the image at different power levels respect to the maximum. In particular, the acceptance angle as defined in the standard can be obtained from the width at 5% of the maximum and then, an estimate of the NA can be calculated.

In order to give a more compact characterization of the FFP profiles, the Levenberg-Marquardt algorithm [7, 8] was used to determine the least squares set of coefficients that best fit the given profile to a Super-Gaussian (SG) function given by the following equation:

$$SG(x) = F + A \exp\left\{-\left[\left(\frac{x - x_0}{\sigma}\right)^2\right]^k\right\}$$

being F, A, x_0, σ, and k the parameters to estimate. After analysing the fits to several profiles we realised that the value of x_0 always corresponded to the centroid coordinate. Therefore, the coefficient x_0 was not taken as a variable parameter to fit the profile, but was fixed to the centroid coordinate. The parameters F and A, are related to the background level and the amplitude of the image respectively. From the parameters σ and k, related to the standard deviation and the kurtosis, an estimation of the NA can be straightforwardly calculated. In addition, k gives a direct description of the flatness or sharpness of the profile. This parameterisation of the FFP profiles provides a better insight of the relative contribution of the different modes, and produces a mathematical expression suitable to be introduced in models devoted to predict bandwidth from modal distribution. The mean square error was sufficiently small to guarantee a good agreement between the fitted model and the experimental data.

Results and Discussion

1.Validation of the methods:

In order to assess the correctness of our methods, we have compared our results with those obtained with the JIS. Thus, we also estimated the exit NA using a horizontal scanning of the FFP. After displacing the screen, the fibre output power was measured with the silicon detector scanning the output angle in 2 degree steps in the horizontal dimension. Thus, the horizontal profile obtained from the FFP image and the one measured by the scanning method can be compared under the same conditions. Figure 2 shows as an example the profiles corresponding to a 5m fibre when the source was the laser and no scrambler was used. Data points are the measurements obtained with the detector and the line is the raw horizontal profile extracted from the 2D FFP image. One can see that both profiles are similar apart from the noise. The NAs derived from the data were of 0.3217 for our method, and of 0.3316 for the standard. The differences obtained were proved not to be statistically significant. Profiles obtained under other conditions were also compared to the standard, always showing insignificant differences.
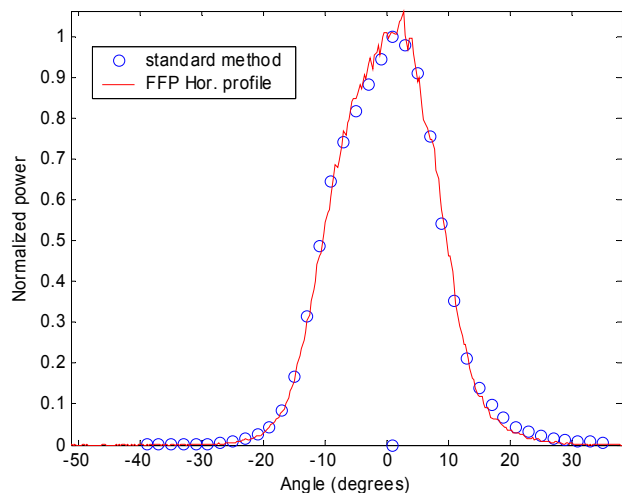

Figure 2: Comparison of the horizontal profiles extracted from the 2D FFP (lines) and measured by the scanning method (data points) for a 5m fibre using a laser source without scrambler.

2. Comparison of the NA estimation methods

In the last section, we described several methods to estimate the NA from the FFP image. First, the acceptance angle was obtained directly from the horizontal and radial profiles (HP and RP, respectively). Then, the acceptance angle was defined as the radius of the circle containing the pixels with more than 5% of the maximum (2D). Finally, it was calculated from the parameters σ and k of the Super-Gaussian fit to the
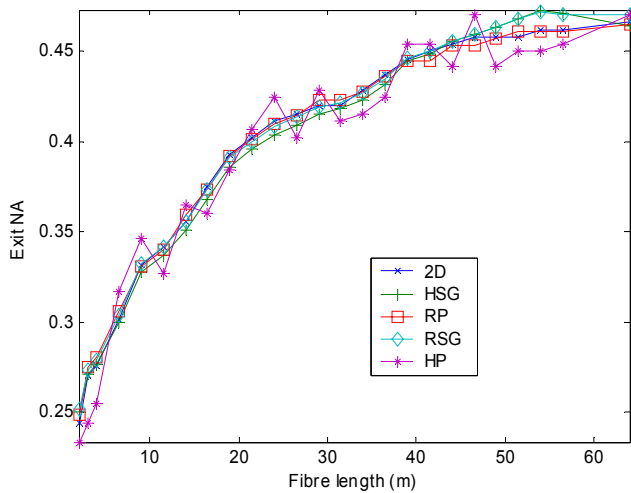
Figure 3: NA versus fibre length obtained using a laser source without scrambler.

horizontal and radial profiles (HSG and RSG). Figure 3 shows NA versus length for one of the conditions (laser source without scrambler), obtained by the 5 methods using different symbols. It is evident from the figure that the scatter in the data from different methods is not large and that there is not a particular bias in any of the estimates. To confirm this later point, we have obtained the mean and standard deviation of the difference of each of the estimates relative to the others. Our calculations show that the NA obtained from the fit of the radial profile has the smallest standard deviation, and thus, we will use this method for the following analysis. The difference with the other methods is, however, very small which confirms that none is significantly biased. The calculation of the NA from the raw horizontal profile exhibits the highest standard deviation, due to the fact that this profile is the noisiest as no filtering or smoothing has been applied to the data.

3. NA versus length for different launching conditions

One of the aims of this study is to analyse the influence of the launching conditions in the exit NA and to determine its dependence with length. Thus, in Figure 4 the NA estimated from the Super-Gaussian fit to the radial profile is represented for the four launching conditions. The figure shows that at the shortest fibre length (2m) there are marked differences between the four launching conditions. When using the laser, the power is launched only in the central modes and the light power is hardly spread to higher order modes after only 2 meters. The situation is the same in the other conditions, but the starting values are greater when the source is the led or when a scrambler is used with any of the sources. The

Figure 4: NA versus fibre length for different launching conditions.

NA obtained with the laser when using the scrambler is also smaller than that obtained with the led with scrambler. The data for the conditions with the scrambler are rather noisy particularly for short distances as they are very sensitive to differences in the position and insertion of the scrambler. The exit NA versus length for the conditions with the scrambler is not flat but increases with distance up to 30-40 meters, although more smoothly than for the other conditions. This fact suggest that for this two relatively narrow sources the spreading induced by the scrambler is not enough to reach an stationary value for the NA at short distances. When the light travels longer distances

inside the fibre, modal coupling produces power transfer to outer modes and the NA increases consequently. At fibre lengths above 50m, the differences between the four conditions become practically insignificant.

4. Variation of the FFP profiles with fibre length

Figures 5a and 5b show the FFP image, the contour plot and the fit to the horizontal profile when the source was an unscrambled laser for fibre lengths of 56.5m and 4m. The figures allow us to compare the two FFP images, illustrating that there are not only differences in the size, but also in the shape of the FFP after the light has travelled in the fibre for different lengths. The initial FFP profile looks like a smoothed square pulse, but at the longest distances the FFP looks like a Gaussian distribution. In the contour plot, we can see that the central part is similar for the two fibre lengths, but that the outer spread is considerably larger for the longer fibre.

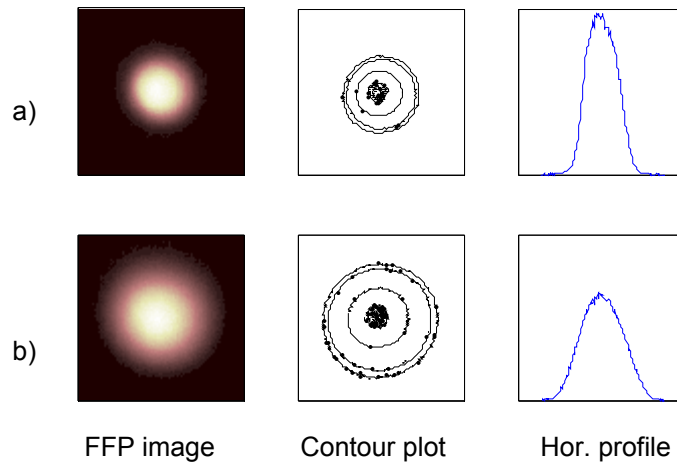FFP image   Contour plot   Hor. profile

Figure 5: FFP images, contour plots, and horizontal profiles obtained with an unscrambled laser source. a) Fibre length of 4m. b) Fibre length of 56.5m.

These differences in shape can be better quantified by using the width at 5%, 10%, 50%, 90% and 95%, which are depicted in Figures 6a, and 6b for the two unscrambled launching conditions. Both figures show that the widths at 90% and 95% are practically constant for the whole range, while the widths at 10% and 5% present an increase with length which is quite steep below 10m. The width at 50% also increases
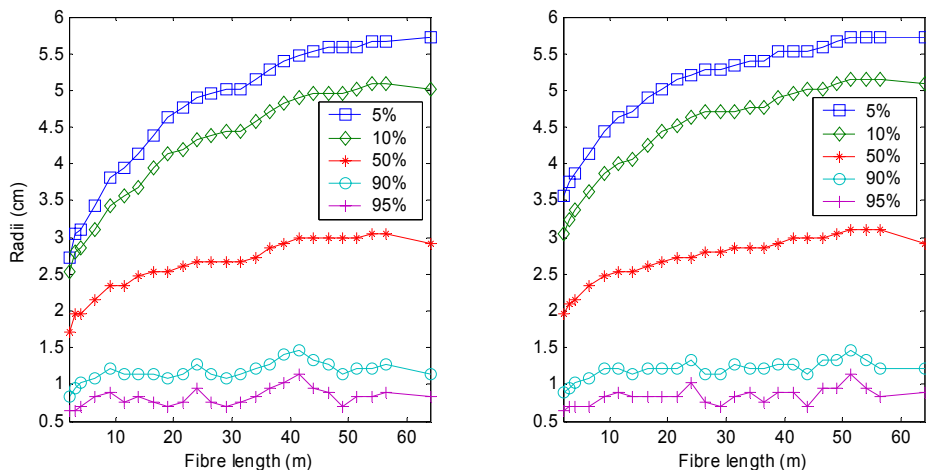

Figure 6: Width versus length at 95%, 90%, 50%, 10% and 5% of the maximum. a) laser without scrambler. b) led without scrambler.

with fibre length, but more smoothly than the later. These results again suggest that there are little changes in the central part of the FFP, and that the power fall at the sides of the centre gets less steep with increasing fibre length. The curves for the scrambler conditions are not shown as they are noisier and flatter that those shown in the figure only showing a very smooth increase with length for the widths at 10% and 5%.

From these results, we can assume that, right after launching, the power is more closely linked to the inner modes, with little power at outer modes. The wider tails found for the led at short distances suggest that the initial modal spread depends on the NA of the source. These tails are even wider for the conditions with scrambler that forces power transfer to outer modes. The power transfer performed by the scrambler in a very short fibre length is equivalent to that produced as the light travels several meters through the fibre, and at the longest distances the stationary shape is reached. This transfer, however, hardly affects the central modes. This effect can be better quantified by using the parameters for the Super-Gaussian fit, and analysing their variation with distance. We have studied this variation and found that the dependence of the standard deviation (σ) is very similar to that of the NA already analyzed. The parameter k, however, offers new information as to the shape of the FFP. When the value of k equals one, the Super-Gaussian becomes a Gaussian. For values higher than one, its shape tends more to a square distribution, and for values smaller than one, it looks like a sharpened distribution. In Figure 7, the kurtosis k of the fit to the radial profiles is represented for the four conditions. The value of k tends to one with increasing distance, indicating that the stationary shape of the FFP is Gaussian-like. The differences in k for the four launching conditions at 2 meters are even larger than those found for the NA. The higher value found in the later case for the unscrambled laser is consistent with its low aperture that only permits the launching of power in very confined modes. For the scrambler launching conditions, the variation of this parameter is again rather flat. These changes in the kurtosis can be explained by modal coupling that causes power transfer from inner to outer modes throughout the fibre.
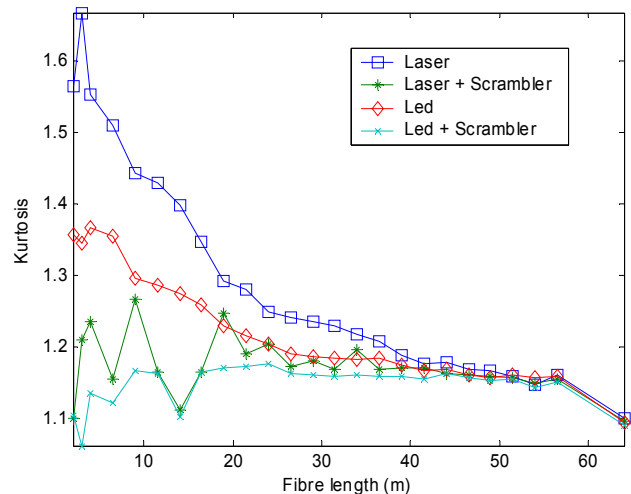

Figure 7: Kurtosis of the Super-Gaussian fit to the radial profile for the four launching conditions

Conclusions

We propose a method to register the FFP images reflected on a screen and validate it comparing their results with those obtained using the Japanese standard to obtain the NA. We applied this method to measure the FFP versus fibre length for a high NA POF and for different launching conditions. We characterised the FFP profiles using a Super-Gaussian function that allows us to quantify the shape variation with fibre length. We found that the shape of the FFP profile changes with distance for all conditions. For short fibre lengths, we found a confined power distribution that evolves as the light travels through the fibre tending to a Gaussian-like function for fibre lengths over 50 meters.

Acknowledgements

References

[1] S. Takahashi, "Experimental studies on launching conditions in evaluating transmission characteristics of POFs". Proc. Int. Conf. POF'93, 83-85. The Hague, Netherlands, 1993.

[2] D. Kalymnios, "Squeezing more bandwidth into high NA POF", Proc. Int. Conf. POF'99, 18-24. Chiba, Japan, 1999.

[3] Japanese Industrial Standard. Test methods for structural parameters of all plastic multimode optical fibres, JIS C 6862, Japan, 1992.

[4] J. Mateo et al., "High NA POF Dependence of Bandwidth on Fibre Length". Proc. Int. Conf. POF'2003, pp. 123-126. Seattle, USA 2003.

[5] G. Fuster, D. Kalymnios, "Passive components in POF Data Communications". Proc. Int. Conf. POF'98, pp. 75-80. London, UK, 1998.

[6] Far Field Pattern Measurement of POF in the Presence of Speckle Noise, Proc. Int. Conf. POF'2003, Seattle, USA 2003.

[7] Levenberg, K., "A Method for the Solution of Certain Problems in Least Squares," Quart. Appl. Math, Vol. 2, pp. 164-168, 1944.

[8] Marquardt, D., "An Algorithm for Least Squares Estimation of Nonlinear Parameters," SIAM J. Appl. Math, Vol. 11, pp. 431-441, 1963.

Contact address

M. A. Losada
Centro Politécnico Superior
María de Luna, 3
50018 Zaragoza, Spain

Phone #:34 976 76 23 73
Fax #:34 976 76 21 11

e-mail: alosada@unizar.es